Topical Meeting on Integrated Photonic Research (IPR '98), 1998 Technical Digest Series
(Optical Society of America ,Washington, D.C., 1998), Vol. 4, p. 304

Integrated Optical Ti:Er:$LiNbO_3$ DBR-Laser with Fixed Photorefractive Grating

CH. BECKER, A. GREINER, TH. OESSELKE, A. PAPE, W. SOHLER, H. SUCHE

Universität-GH Paderborn, Angewandte Physik
Warburger Straße 100, D-33098 Paderborn, Germany
Fax: +49-5251-603422; e-mail: suche@physik.uni-paderborn.de

Introduction: Recently, integrated optical Ti:Er:$LiNbO_3$ DBR-(Distributed Bragg Reflector-) lasers have been developed with holographically defined ion beam etched surface grating for narrowband optica feedback [1]. However, DBR-lasers with etched surface gratings suffer from several drawbacks: The fabrication technology is complicated [2]. Grating inhomogeneities induce extra losses of the lasing mode The overlap of the grating and the lasing mode is very small requiring a long interaction length. The pum mode is partially coupled to substrate modes resulting in high extra losses; therefore, pumping through th Bragg-grating is not possible.
Photorefractive gratings, as sucessfully used in fiberoptic DBR- and DFB-lasers [3], are a very promising alternative, avoiding all the drawbacks mentioned above. We report in this contribution the first DBR-waveguide laser (λ = 1531nm (and λ = 1546nm)) in Er-diffusion-doped $LiNbO_3$ with a fixed photorefractive grating in an Fe-doped Ti-diffused strip waveguide; the device is pumped by a laser diode ($\lambda \approx$ 1480nm).

Laser Fabrication: A schematical diagram of the laser is presented in Fig. 1. It is fabricated in a 70mm long X-cut $LiNbO_3$ substrate, which has been Er-doped over 43mm by an indiffusion of a 15nm thick, vacuum-deposited Er-layer at 1120°C during 120h. Subsequently, the remaining surface has been iron-diffusion doped (33nm, 1060°C, 72h) to increase the photorefractive sensitivity for grating fabrication. Finally, a 8µm wide, 97nm thick, photolithographically defined Ti-stripe parallel to the c-axis has been indiffused forming the optical channel guide. The sample has been annealed at 500°C for 3h in flowing Ar (0.5l/min) to enhance the Fe^{2+}/Fe^{3+}-ratio, which determines the photorefractive susceptibility.

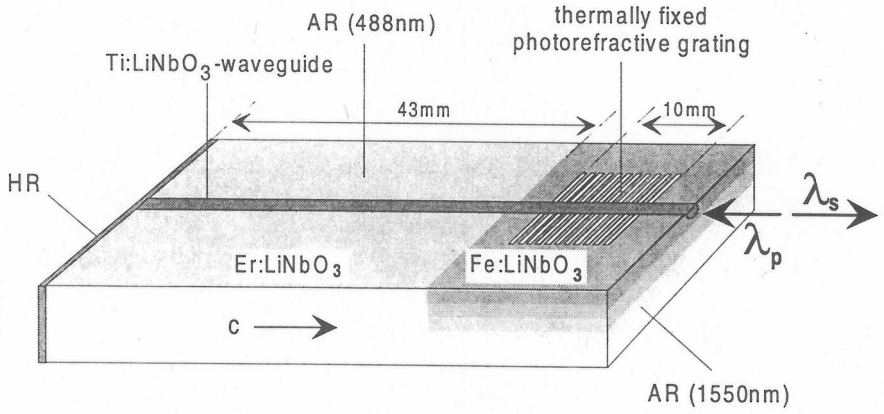

Fig. 1: Schematical structure of the Ti:Er:$LiNbO_3$ DBR waveguide laser with photorefractive grating in the Fe-doped section. HR: Highly reflecting dielectric mirror; AR: anti-reflection coating.

The laser resonator consists of a broadband dielectric high reflector on the polished waveguide end face o the Er-doped section. The end face of the Fe-doped section has been antireflection coated for fibre butt coupling. Finally, the upper and lower sample surfaces have been AR-coated to avoid interference effects during the grating writing.

The grating has been written using a holographic setup with the 488nm line of an Ar-laser. The periodic illumination leads to a corresponding excitation of electrons from Fe^{2+}-states; they are redistributed by drift, diffusion and the photovoltaic effect in $LiNbO_3$. The latter is the dominant transport mechanism along the optical c-axis. Finally, the electrons are trapped by acceptor states (Fe^{3+}-ions) in areas of low optical intensity. This redistribution generates a periodic space charge field which modulates the refractive inde via the electrooptic effect and generates in this way a narrowband Bragg-reflector grating.
A grating fabricated at room temperature is not stable. Therefore, it has been written by a 2-hours exposure at 170°C. At this temperature protons in the crystal become mobile and compensate the periodic electronic space charge [4, 5]. After cooling to room temperature, these ions are frozen at their high temperature positions. Homogeneous illumination with the collimated beam of a 100 W halide lamp then leads to a nearly homogeneous redistribution of the electronic charge, developing in this way a stable ionic grating as a replica of inverse polarity of the initial electronic space charge distribution.

Laser Properties: The laser has been first characterized as passive device. The erbium and the iron concentration profiles are Gaussian-like with surface concentrations of $1.15 \cdot 10^{20}(3.3 \cdot 10^{19})cm^{-3}$ and 1/e-penetration depths of 4.7(63)µm for Er(Fe), respectively.
The Ti-diffused optical waveguide is single mode for wavelengths around 1550nm, with the fundamental TM-mode slightly larger than the TE-mode (8.5µm(width) × 4.8µm(depth) and 8.4µm × 4.5µm, respectively). The scattering losses are as low as 0.02dB/cm in a reference channel without Er-doping. For the Er-doped waveguide scattering losses of about 0.2dB/cm are estimated by the comparison of modelled and measured laser results. Absorption coefficients for the Er-doped section have not been measured, but can be estimated to be about 1.4(8.5)dB/cm at 1480(1531)nm wavelength for TE-polarised light. These values can be inferred from mode-size and absorption cross section measurements for α-polarised light.

The high reflector has reflectivities of about 80% for both, signal- and pump wavelengths. In this way double pass pumping of improved absorption efficiency is achieved. The spectral characteristics of the holographically written grating has been determined by slightly pumping the device and measuring the backscattered amplified spontaneous emission from the Er-doped section transmitted through the grating. This yielded a minimum transmission of about 40%, corresponding to a reflectivity of about 60%. Due to an electronic compensation of the ionic grating the reflectivity drops slowly as function of time. However, this compensation can be easily reversed by homogeneous illumination. Fig. 2 shows the specific result measured for the optimum output coupling of the DBR-laser. The halfwidth of the grating is about 0.11nm.

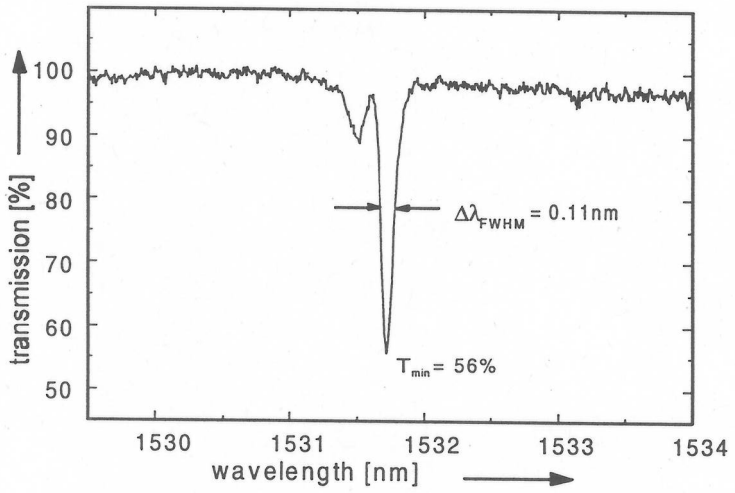

Fig. 2: Transmission of a fixed grating after homogeneous illumination versus wavelength.

To operate the DBR-laser, a pigtailed diode laser ($\lambda_p \approx 1480$nm) has been used for pumping. A fiberoptic wavelength division multiplexer (WDM) launched up to 110mW of pump power into the DBR-laser and simultaneously extracted the laser emission in backward direction.

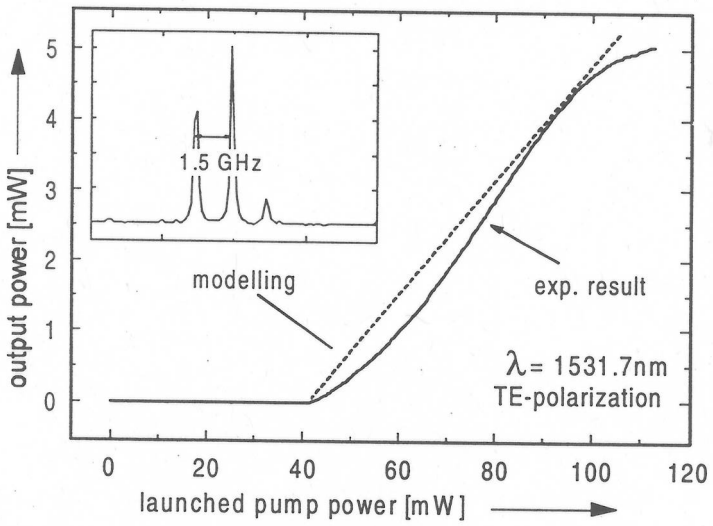

Fig. 3: Power charcteristics of the DBR-laser. Inset: axial mode spectrum (TE-polarised).

Laser emission could be achieved in both, TE- and TM-polarisation. The actual polarization was determined by the location of the axial eigenmodes with respect to the peak reflectivity of the Bragg reflector. By thermal drift alternating TE- and TM-emission could be observed, respectively. TE-polarization for both, pump and emission, has yielded the maximum output power (see Fig. 3), as the smaller TE-modes result in a better overlap with the erbium concentration profile. To suppress TM-emission, a stripe of silver paste operating as a TE-pass polarizer has been deposited across the waveguide close to the high reflector. The bandwidth of the grating of ≈ 0.11nm has led to the simultaneous emission of three longitudinal modes (see inset of Fig. 3) with a central wavelength of 1531.7nm. The output power of the DBR-laser has been monitored as function of the reflectivity of the Bragg grating, starting with a reflectivity of about 60%. The maximum TE-polarized output power of 5.1mW has been measured for a grating reflectivity of about 45%.
Modelling results predict a significant potential for improvements. Assuming 0.1dB/cm waveguide scattering losses, an optimized Er-diffusion and output coupling through the grating, up to 32% slope efficiency and 15mW output power at 80mW of launched pump power seem to be feasible at the same emission wavelength.

Acknowledgement: We thank Prof. Krätzig and Dr. Kip of the University of Osnabrück, Germany, for helpful discussions about the photorefractive effect and for vacuum depositing the Fe-layers needed for diffusion doping.

References:

[1] J. Söchtig, R. Groß, I. Baumann, W. Sohler, and H. Schütz, R. Widmer, Electron. Lett., **31,** pp. 551-552 (1995)
[2] J. Söchtig, H. Schütz, R. Widmer, H.W. Lehmann, R. Groß: Proc. SPIE Conf. on Nanofabrication and Device Integration, **2213**, pp. 97-98 (1994)
[3] J. Hübner, P. Varming, and M. Kristensen, Electron. Lett. **33** (2), pp. 139-140 (1997)
[4] J.J. Amodei, D.L. Staebler, Appl. Phys. Lett., **18**, pp. 540-542 (1971)
[5] Buse, K., Breer, S., Peithmann, K., Kapphan, S., Gao, M., Krätzig, E.: Phys. Rev. (B), **56** (3), pp. 1225-1235 (1997)